

Euler Deconvolution Technique for Magnetic Source-depth Determination Using Aeromagnetic Data

¹Adegoke, J.A. and ²Layade, G.O.

¹Department of Physics, University of Ibadan, Nigeria

²Department of Physics, Federal University of Agriculture, Abeokuta Nigeria.

Abstract

An automated 2-D Euler deconvolution method was applied on a digitized aeromagnetic data for Ogbomoso area with sheet number 221 in order to determine depth to basement, horizontal position of the object and possible geometry base on the structural index of 0-3 so as to describe the body as contact, thin dyke/sheet, vertical/horizontal cylinder or sphere within the bedrock. The surveyed area falls within longitudes 4°00' E and 4°30' E and latitudes 8°00' N and 8°30' N which covers the distance of 55 km by 55 km (3025 km²). The data acquired, gridded and delineated into profiles at 100 m interval. Filtering process was applied to remove the regional gradient and other possible magnetic noises. Reduction-to-pole of the total magnetic field intensity was carried out; the contour map and surface distribution of the magnetic minerals was obtained using semi-automated geophysical software. The results yielded both minimum and maximum values with 35.11m and 53.93 m for contact, 360.08 m and 548.29 m for thin sheet, 721.16 m and 1093.90 m for cylinder, while sphere has the depth of 1082.23 m and 1646.87 m respectively. Qualitatively, the magnetic mineral distribution follows SW-NE path of the location.

Keywords: Aeromagnetic data, profile, Ogbomoso, anomaly, deconvolution, geometry

1.0 Introduction

Airborne geophysical surveys are an extremely important aspect of modern geophysics compared with ground surveys. Airborne surveys allow faster and usually cheaper coverage, of large areas [1]. The stages of magnetic data interpretation generally involve the application of mathematical filters to observed data. The specific goals of these filters vary, depending on the situation. The general purpose is to enhance anomalies of interest and/or to gain some preliminary information on source location or magnetization.

One important goal in the interpretation of magnetic data is to determine the type and the location of the magnetic source. This has recently become particularly important because of the large volumes of magnetic data that are being collected for environmental and geological applications. Consequently, a variety of semiautomatic methods, based on the use of derivatives of the magnetic field, have been developed to determine magnetic source parameters such as locations of boundaries and depths [2], [3].

As faster computers and commercial software have become widely available, these techniques are being used more extensively. Utilizing first-order derivatives of the magnetic field, Euler deconvolution was first presented for profile data [4] and for gridded data [5]. The main advantage of the Euler method is that it can provide automatic estimates of the source location of the causative magnetic anomalies.

However, it requires an assumption about the type of body that is, the source. In practice, this is achieved by specifying a structural index (η) to define the source type in generalized situations, setting a good strategy for discriminating, and selecting meaningful solutions. Recent extensions to the Euler method allow η to be estimated from the data, with the calculation of Hilbert transforms of the derivatives [6].

Very recently, several new approaches have been developed that deal with depth determination and structural index estimation simultaneously. One method [7] calculates the field at many altitudes and scales the field by a power law of the altitude. The depth and index can be obtained by finding extreme points. Another method [8] assumes (like the Euler method) homogeneous potential fields, but applies a similarity transform. The enhanced local wavenumber method (ELW) for interpreting profile magnetic data was also presented for determining depth [9]. The 2D Euler equation [4] showed that deconvolution of the derivatives of the local phase can provide automatic estimates of the source location regardless of the nature of the sources.

Corresponding author: Layade, G.O., E-mail: layadeoluyinka018@gmail.com, Tel.: +2348139437356

2.0 Materials and Method

2.1 Location of the Study Area

Ogbomoso is a city in Oyo State, southwestern Nigeria, on the A1 highway. It was founded in the mid-17th century. The population was approximately 645,000 as of 1991; as of March 2005, it is estimated to be around 1,200,000. The majority of the people are members of the Yoruba ethnic group. Yams, cassava, maize, and tobacco are some of the notable agricultural products of the region.

Ogbomoso is located on Latitude $8^{\circ} 08' 00''$ and Longitude of $4^{\circ} 16' 00''$ North of the Equator. Ogbomoso, the second largest City in Oyo State after Ibadan, which is the Capital of Oyo State, lies within the derived savannah region and it is a gateway to Northern part of Nigeria from the West. Ogbomoso is 57 Kilometers South West of Ilorin (the Capital of Kwara State) 53 Kilometers North – East of Oyo, 58 Kilometers North – West of Osogbo (Capital of Osun State) and 104 Kilometers North – East of Ibadan (Capital of Oyo State)

Ogbomoso lies in the transition zone forest of Ibadan Geographical region and the Northern savannah region. As a result of this, it is regarded to be of derived savannah vegetation. The Town is seen to be a low land forest Area with Agricultural activities being the major activities carried out on it. The regions around and within Ogbomoso has four seasons like most of the other area in the southern Nigeria. The long wet season starts from March to July; it is the season of heavy rainfall and high humidity. The short dry season is normally in August. This is followed by short wet season and last September to October. The last season is that of harmattan experienced at the end of November to mid-March. The man annual rainfall is 1-24mm. The variation in rainfall quantities between different between stations is rather in significant both on an annual and monthly basis.



Figure 1: Map of the Location of the study area.

2.2 Geology of the study Area

The geology of Ogbomoso (Fig. 2) consists of Precambrian rocks that are typical for the basement complex of Nigeria [10]. The major rock associated with Ogbomoso area form part of the Proterozoic schist belts of Nigeria, which are predominantly, developed in the western half of the country. In terms of structural features, lithology and mineralization, the schist belts show considerable similarities to the Achaean Green Stone belts. However, the latter usually contain much larger proportions of mafic and ultramafic bodies and assemblages of lower metamorphic grade [10].

The gneiss complex which underlies the northern and southern part of the Ogbomoso district comprises a considerable broader area of outcrops. Locally, the rock sequence composes of basically weathered quartzite and older granites. The minerals found in this area constitute mostly amphibolites, amphibole schist, meta ultra mafites and meta pelites. Extensive psammitic units with minor metapelite can also be found. These consist of quartzites and quartz schist. All these assemblages are associated with migmatitic gneisses and are cut by a variety of granitic bodies [10].

The rocks of the Ogbomoso district may be broadly grouped into gneiss-migmatite complex, mafic-ultra mafic suite (or amphibolite complex), meta sedimentary assemblages and intrusive suite of granitic rocks [11]. A variety of minor rock types are also related to these units. The gneiss-migmatite complex comprises migmatic and granitic, calcareous and granulitic rocks. The mafic-ultramafic suite is composed mainly of amphibolites, amphibole schist and minor metaultramafites, made up of anthophyllite-tremolite-chlorite and talc schist [12]. The meta sedimentary assemblages, chiefly meta pelites and psammitic units are found as quartzites and quartz schist. The intrusive suite consists essentially of Pan African (c.600Ma) Granitic units. The minor rocks include garnet-quartz-chlorite bodies, biotites-garnet rock, syenitic bodies, and dolerites [10],[13].

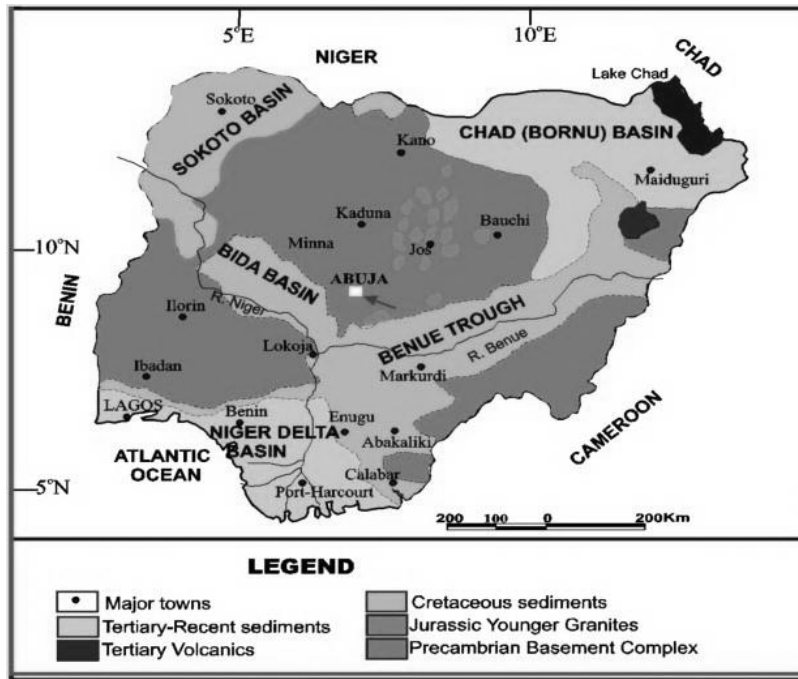


Fig. 2: Geological map of Nigeria

2.3 Data Correction and Filtering

The digitized aeromagnetic data of Ogbomoso area with sheet no 221 which covers the total area of 55 km by 55 km was processed and transformed into profiles. The transformed data was then converted into an executable grid format through the use of Golden Surfer. The data was filtered in order to remove the regional gradient and magnetic noise. Kriging approach was used to grid the data from which the coloured map of the location was generated in Figure 4.1 which shows the magnetic intensity values of the area in nanotesla. The area was contoured at the magnetic interval of 40 nT.

Furthermore, the reduction to pole was performed to simplify the interpretation of anomalies by removing the asymmetry introduced due to its induction by the inclined main field. The main field in only vertical at the north and south magnetic poles. As the name implies reduction to pole transform the data to that which would be measured at the magnetic poles. This simplifies the anomalies by centering anomalies over the causative magnetic body rather than being skewed and offset to one side.

2.4 The Euler Deconvolution

Thompson [4] proposed a technique for analyzing magnetic profiles based on Euler’s relation for homogeneous functions. The Euler deconvolution technique uses first-order x , y and z derivatives to determine location and depth for various idealized targets (sphere, cylinder, thin dike, contact), each characterized by a specific structural index. Although theoretically the technique is applicable only to a few body types which have a known constant structural index, the method is applicable in principle to all body types. The technique is extended to 3D data by applying the Euler operator to windows of gridded data sets [5]. The applicability of the technique was further simplified to handle spatial data using the indexes [14], [15].

Magnetic field M and its spatial derivatives satisfy Euler’s equation of homogeneity,

$$(x - x_0) \frac{\partial M}{\partial x} + (y - y_0) \frac{\partial M}{\partial y} + (z - z_0) \frac{\partial M}{\partial z} = -NM \tag{1}$$

Where $\frac{\partial M}{\partial x}$, $\frac{\partial M}{\partial y}$, and $\frac{\partial M}{\partial z}$ in equation (1) represents first order derivative of the magnetic field along x -, y -, and z -

directions, respectively. N is known as a structural index and related to the geometry of the magnetic source. For example, $N=3$ for sphere, $N=2$ for pipe (cylinder), $N=1$ for thin dike and $N=0$ for magnetic contact [5]. Taking into account the base level for the regional magnetic field B , equation (1) can be rearranged and written as,

$$x_0 \frac{\partial M}{\partial x} + y_0 \frac{\partial M}{\partial y} + z_0 \frac{\partial M}{\partial z} + NB = x \frac{\partial M}{\partial x} + y \frac{\partial M}{\partial y} + z \frac{\partial M}{\partial z} + NM \tag{2}$$

Assigning the structural index (N), a system of linear equations is obtained and solved for estimating the location and depth of the magnetic body. Using a moving window, multiple solutions from the same source can be obtained. Good solutions are considered to be those that cluster well and have small standard deviations [4],[5].

The Quantitative interpretation of the data was carried out using a software-*Euler Deconvolution for Windows* developed by G.R.J Cooper (2000) of Geosciences Department, University of the Witwatersrand, Johannesburg, South Africa. This was used to model the Total Magnetic, Reduction-to-pole, Horizontal and Vertical Gradient of the anomaly. The Qualitative interpretation of magnetic data set is primarily hinging on map based recognition of features such as: discrete intrusion, discontinuities/offsetting fault, structural styles, disruptive cross-cutting features, tectonic events, basement terrains, sediment pathways, and depocentres[16].

The automated application is a window based which operates on atwo-stage process. The input and the output levels through which the gridded data is loaded into the system. This window enables the user to control and specify the type of the data as magnetic, gravity or analytical signal. Also, the geomagnetic intensity value, angle of inclination, declination and flight are specified. The output plots are generated for reduction to pole, total magnetic intensity, horizontal and vertical derivatives respectively in the same window. The output is then used to determine the depth with clustered points gives the best result as showing in Figs. 3-7

3.0 Result and Discussion

The results along five profiles were considered within the locality as shown in Table 1.

Table 1: Range of Depth (m) to the Magnetic Source of the Geometrical Model

Profile	Depth (m)			
	Contact	Thin Dyke/Sheet	Cylinder (horizontal/vertical)	Sphere
A-A*	44.43-44.70	453.28-456.04	907.56-913.08	1361.84-1370.12
B-B*	50.27-53.93	511.74-548.29	1024.49-1093.90	1563.0-1646.87
C-C*	37.38-38.19	386.62-388.38	774.24-782.76	1161.11-1174.64
D-D*	35.11-35.37	360.08-362.71	721.16-726.42	1082.23-1090.13
E-E*	49.46-49.57	503.59-504.68	1008.18-1010.35	1512.77-1516.03

In a quantitative manner, the profile A-A* in Figure 3 reveals various magnetic spikes of different signatures for the reduction to pole data. However, a close observation of the anomaly indicated that the maximum magnetic signature occurred at the horizontal position 27500 m along the profile. The calculation of the magnetic depth to the edge of the source was done with the following results as shown in Table 1. The four possible geometry following the 2D Euler equations gives contact the depth range of 44.43 – 44.70 m, thin sheet/dyke revealed 453.28 – 456.04 m, and cylinder indicated the depth of 907.56 – 913.08 m while the magnetic source with spherical index has the depth range of 1361.84 – 1370.12 m respectively.

The magnetic signatures in Figure 4 of the Euler deconvolution method has a significant shape which spread across the profile B-B* within the 7000 m horizontal distance. However, with the structural indices of the equations, it is obvious that the magnetic minerals were distributed almost evenly along the profile with various depths to the source top as 50.27 – 53.53.93 m was found for contact, 511.74 – 548.29 m for thin sheet/dyke, both horizontal and vertical cylinder has 1024.49 – 1093.90 m depth and 1563.0 – 1646.87 m was calculated for the sphere.

The Figures 5 and 6 which showing profile C-C* and D-D* reveal almost the same pattern of magnetic mineral surface distribution on the 2D Euler deconvolution plots. By physical inspection along the 55000 m profile length, there are sprockets of magnetic anomaly of the reduced to pole data with minimum and maximum respectively. The result of the analysis of the profiles reveal the following for profile C-C*; the depth to the top of the magnetic source of the basement complex for contact source is 37.38 – 38.19 m, 386.62 – 389.19 m for thin sheet/dyke, 774.24 – 782.76 m for cylinder and 1161.11 – 1174.64 m in profile C-C* while profile D-D* has contact, thin sheet/dyke, cylinder and spherical sources produced the depth range of 35.11 – 35.37 m, 360.08 -362.71 m, 721.16 – 726.42 m and 1082.23 – 1090.13 m respectively.

The profile E-E* along horizontal distance produced substantial magnetic signatures with the distribution follows the decay function as the profile progresses. The information provided by Figure 7 and Table 1 shows that the depth range of 49.46 – 49.57 m was for contact surface, 503.59 – 504.68 m for thin sheet/dyke, 1008.18 -1010.35 m for cylindrical source and 1512.77 – 1516.03 for sphere respectively.

As the magnetic anomaly could be better interpreted both in quantitative and qualitative approach, hence the essence of Figures 8,9,10. The total magnetic intensity of the area was mapped at 40 nT interval with the resulting magnetic mineral distribution is shown in Figure 8, also the 3D surface distribution of the mineral in the locality was generated by golden surfer as shown in Figure 9 while a gridded contour map of the magnetic anomaly was generated which shows the distribution along stretch of SW-NE of the locality.

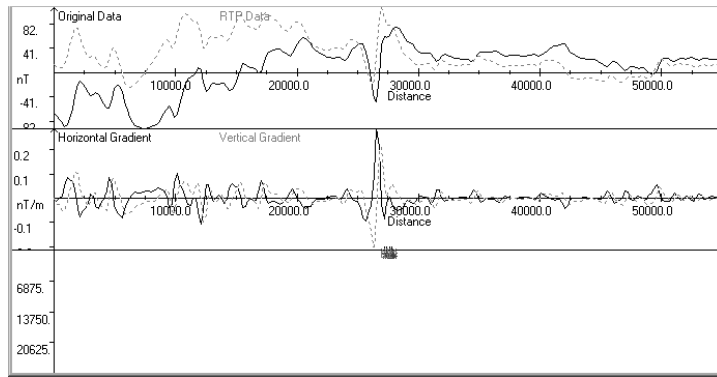


Figure 3: Euler Deconvolution output for the magnetic depth determination along profile A-A*

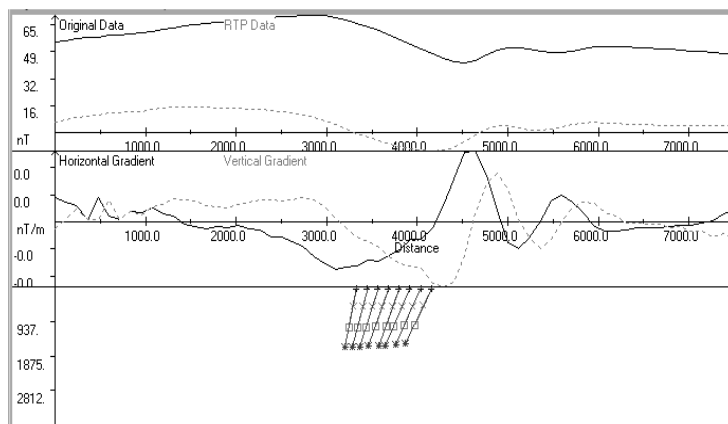


Figure 4: Euler Deconvolution output for the magnetic depth determination along profile B-B*

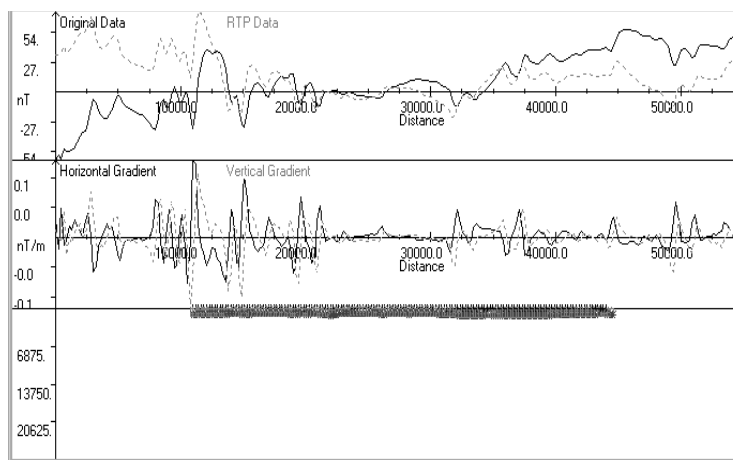


Figure 5: Euler Deconvolution output for the magnetic depth determination along profile C-C*

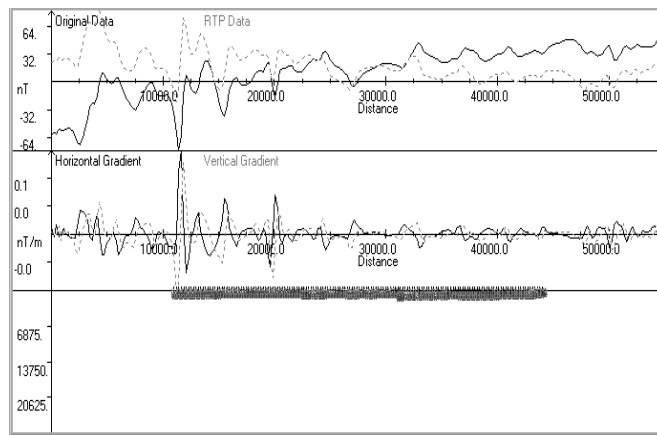


Figure 6: Euler Deconvolution output for the magnetic depth determination along profile D-D*

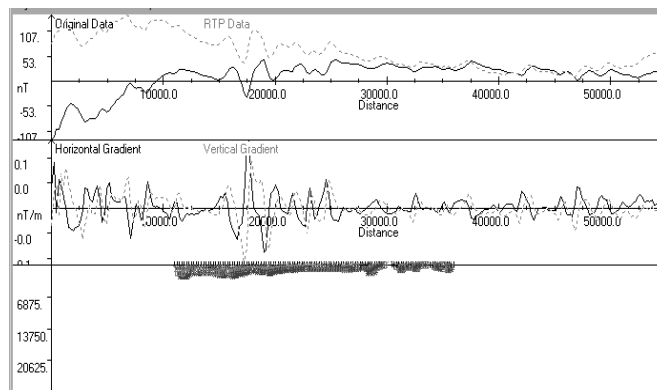


Figure 7: Euler Deconvolution output for the magnetic depth determination along profile E-E*

CONTOUR PLOT OF MAGNETIC RESIDUAL ANOMALY OF IRON-ORE DEPOSIT IN OGROMOSO AREA USING AIRBORNE DATA

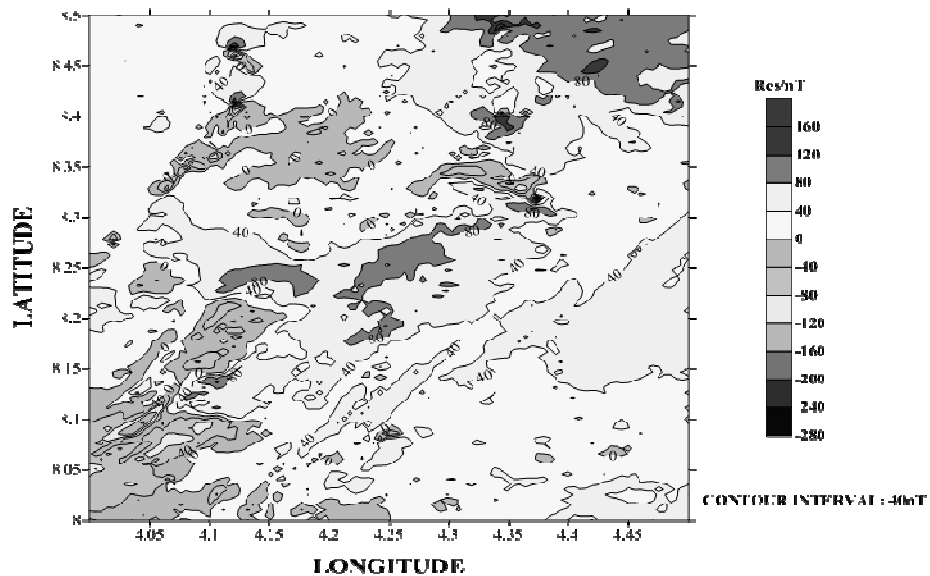


Figure 8: Contour plot of the Residual anomaly map of the area

3D SURFACE DISTRIBUTION OF MAGNETIC RESIDUAL ANOMALY OF IRON-ORE DEPOSIT IN OGBOMOSO AREA USING AIRBORNE DATA

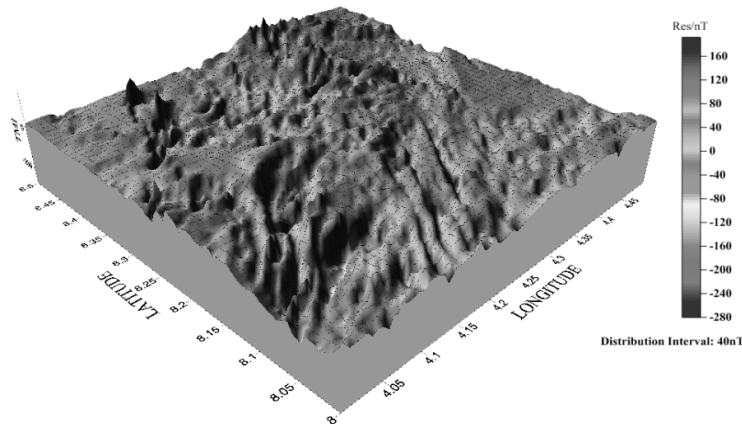


Figure 9: 3D-Surface distribution of the magnetic mineral in the locality

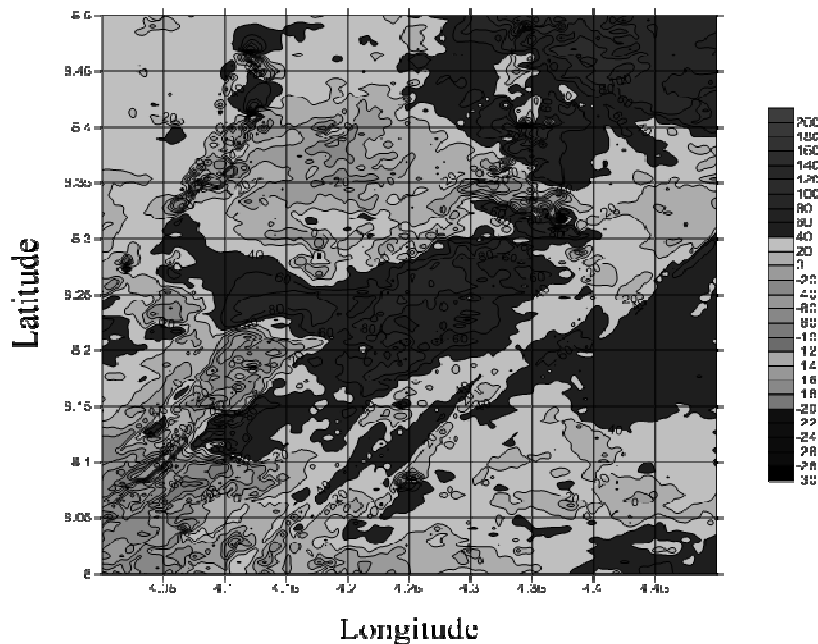


Figure 10: A gridded contour map of the study area in Geographical coordinates.

4.0 Conclusion:

The aeromagnetic data of some part of ogbomosohas been analysed with the aid of 2D Euler deconvolution method on the basis of its structural indices of value 0-3 which characterize the magnetic mineral sources as contact, thin sheet/dyke, cylinder and sphere respectively.

The distribution of magnetic minerals spread across the geographical coordinates of the area with depth to top of the magnetic source was found having both minimum and maximum value corresponding to the prospect of the area in the geomagnetic mineral exploration.

The subsurface structures within the basement complex of ogbomososo were mapped with the spread of minerals along SW-NE zone of the entire area under investigation.

References

- [1] Horsfall, K.R., 1997. Airborne Magnetic and Gamma-Ray data Acquisition. AGSO journal of Geology and Geophysics 17:23-30
- [2] Blakely, R. J., 1995, Potential theory in gravity and magnetic applications: Cambridge University Press.

- [3] Nabighian, M. N., V. J. S. Grauch, R. O. Hansen, T. R. LaFehr, Y. Li, J. W. Peirce, J. D. Phillips, and M. E. Ruder, 2005, The historical development of the magnetic method in exploration: *Geophysics*, 70, no. 6, 33ND–61ND.
- [4] Thompson, D. T., 1982, EULDPH: A new technique for making computer assisted depth estimates from magnetic data: *Geophysics*, 47, 31–37.
- [5] Reid, A. B., J.M. Allsop, H. Granser, A. J. Millet, and I.W. Somerton, 1990, Magnetic interpretation in three dimensions using Euler deconvolution: *Geophysics*, 55, 80–91.
- [6] Nabighian, M. N., and R. O. Hansen, 2001, Unification of Euler and Werner deconvolution in three dimensions via the generalized Hilbert transform: *Geophysics*, 66, 1805–1810.
- [7] Fedi, M., 2007, DEXP: A fast method to determine the depth and the structural index of potential fields sources: *Geophysics*, 72, no. 1, I1–I11.
- [8] Stavrev, P., and A. Reid, 2007, Degrees of homogeneity of potential fields and structural indices of Euler deconvolution: *Geophysics*, 72, no. 1, L1–L12.
- [9] Salem, A., D. Ravat, R. Smith, and K. Ushijima, 2005, Interpretation of magnetic data using an enhanced local wavenumber *_ELW_* method: *Geophysics*, 70, no. 2, L7–L12.
- [10] Rahaman, M.A. (1976). Review of the basement geology of southwestern Nigeria, In: KOGBE, C.A. (ed.) *Geology of Nigeria*. Elizabethan Publishing Company. Lagos, 41-58.
- [11] Oyawoye, M.O. (1964). The geology of the basement complex. *Journal of Nigeria Mining, Geology and Metallurgy*. Volume 1, pp. 87-102.
- [12] Jones, H.A. and R.D. Hockey, 1964. The geology of part of Southwestern, Nigeria. *Geol. Surv. Nigeria Bull.*, 3: 101.
- [13] Folami, S L (1992) Interpretation of Aeromagnetic Anomalies in Iwaraja Area. Southwestern Nigeria. *Journal of Mining and Geology* 28 (2) 391-396
- [14] Mushayandebvu, M., A. Reid, and D. Fairhead, 2000, Grid Euler deconvolution with constraints for 2-D structures: 70th Annual International Meeting, SEG, Expanded Abstracts, 398–401.
- [15] Silva, J. B. C., and V. C. F. Barbosa, 2003, Euler deconvolution: Theoretical basis for automatically selecting good solutions: *Geophysics*, 68, 1962–1968.
- [16] Spector A., and Grant F.S., 1970. Statistical Models for Interpreting Aeromagnetic Data. *Geophysics*, 35 pg.293-302.